Journal of Thermal Analysis, Vol. 32 (1987) 393–408

KINETIC ANALYSIS OF THERMAL DEHYDRATION AND HYDROLYSIS OF $MgCl_2 \cdot 6H_2O$ BY DTA AND TG

*Y. Kirsh, S. Yariv** and *S. Shoval***

PHYSICS GROUP, EVERYMAN'S UNIVERSITY, P.O. BOX 39328, TEL-AVIV, ISRAEL
*DEPARTMENT OF INORGANIC AND ANALYTICAL CHEMISTRY, THE HEBREW UNIVERSITY OF JERUSALEM, JERUSALEM, ISRAEL
**GEOLOGICAL GROUP, EVERYMAN'S UNIVERSITY, TEL-AVIV, ISRAEL

(Received November 19, 1985; in revised form June 27, 1986)

The thermal decomposition of $MgCl_2 \cdot 6H_2O$ (non-dried and partly dried) and the kinetics of the process were studied by DTA, TG, DTG, IR, X-ray diffraction and chemical analysis of Mg and Cl. The reactions which occurred in the course of the thermal analysis were identified as dehydration (in steps), thermal hydrolysis of $MgCl_2 \cdot H_2O$ and dehydrochloridization of magnesium hydroxy chlorides. Melting of the phases $MgCl_2 \cdot 6H_2O$, $MgCl_2 \cdot 4H_2O$ and $MgCl_2$ was also identified in the thermal curves. Thermal weight loss continued up to 800 °C in flowing air or nitrogen, but only up to 700 °C in static air. MgO was the end-product of thermal treatment in both cases.

The kinetic parameters of the reaction, the activation energy E, pre-exponential factor A and apparent order of reaction b, were computed by several methods. The activation energy and the apparent reaction order of dehydration were found to increase with decreasing hydration number of the Mg. The dehydrochloridization process had the highest activation energy.

The thermal decomposition of magnesium chloride hexahydrate has recently been the subject of several studies [1–6]. These studies have elucidated some points which were not cleared up in previous work [7–10], especially concerning the influence of the experimental conditions on the dehydration and hydrolysis processes. Very little has been done to determine the kinetic parameters of the reactions, however. In the present study the kinetics of the processes are investigated by applying three methods of analysis to DTA and DTG curves: (1) the method of Freeman and Carroll, (2) the initial rate method, and (3) Chen's "half-width" method. In each of these methods, the activation energy E, pre-exponential factor A and apparent order of reaction b are computed. From a comparison of the results, the reliability of the data can be evaluated. In order to identify the products obtained at various stages of the thermal analysis, infrared

John Wiley & Sons, Limited, Chichester
Akadémiai Kiadó, Budapest

spectra and X-ray diffractograms were recorded after the salt had been heated to various temperatures. In addition, Mg and Cl were determined in the salt treated thermally at various temperatures.

Experimental

Material

$MgCl_2 \cdot 6H_2O$ (Laboratory Reagent) was supplied by BDH. Both non-dried and partly-dried salts were used. The latter was dried for 7 days over 70% sulfuric acid. As will be shown in the next section, in both cases MgO is the end-product of thermal treatment. With this information we could deduce the water content from the total weight loss. The dried and the non-dried samples lost on average 79.25 and 80.70%, respectively, during the thermal analysis, corresponding to $MgCl_2 \cdot 5.5H_2O$ and $MgCl_2 \cdot 6.3H_2O$.

Methods

Thermal analysis

Simultaneous TG, DTG and DTA measurements were carried out in a Stanton Redcroft apparatus (STA 780). Crucibles of alumina or quartz were used both for the specimen and for the reference material, which was calcined alumina. The samples (10 mg of crystalline or powdered salt) were heated from room temperature to 1000°, the heating rate in most cases being 10 deg/min. A few runs were carried out with a lower (2 deg/min) or higher (25 deg/min) heating rate. Measurements were performed in flowing N_2, or in flowing or static air. The temperature was measured near the sample holder by a thermocouple (Pt v. 13% Rh–Pt). The experimental error of the weight losses in the TG curve was about 0.5%, while the mass of the final products could be determined with an accuracy of 0.01%.

Infrared, X-ray and chemical analysis

Non-dried samples were heated in the DTA furnace to various temperatures (heating rate 10 deg/min) and then studied by infrared, X-ray diffraction and chemical analysis. Infrared spectra of the thermally treated samples were recorded in KBr and CsCl disks (1%) with a Perkin–Elmer 597 spectrophotometer after thermal dehydration of the disks.

It has been shown [16] that ion-exchange can take place between $MgCl_2$ and KBr, and therefore CsCl disks were used to detect the $MgCl_2$ in the products of thermal treatment. KBr disks, however, were also useful for studying the OH bands in those products.

The KBr and CsCl disks were dried at 350° and 250°, respectively, in order to drive off the water introduced into the disks during preparation. It has been shown [11] that no thermal hydrolysis of hydrated $MgCl_2$ occurs in CsCl disks during drying, and preliminary experiments showed the same for dilute KBr disks. X-ray diffraction spectra were recorded on a Philips diffractometer. Mg and Cl were determined by titration with EDTA and $AgNO_3$, respectively.

Results and discussion

DTA and DTG peaks below 300°

The thermal curves of the dried and non-dried samples were somewhat different. In the DTA curve of the non-dried samples five distinct endothermic peaks appeared between room temperature and 300°, as shown in Table 1 and Fig. 1. At a heating rate of 10 deg/min, peak *C* was the most intense while peak *A* appeared as a shoulder. Distinct DTG peaks accompanied the last three thermal processes, while the first two appeared only as "shoulders" in the DTG curve. The reproducibility was good, and the shapes of the curves were not dependent upon the type of samples (crystalline or powder) or the atmosphere.

The curves of the dried samples were similar (Fig. 2), but peak *C* was weaker in both the DTA and the DTG curves, and peak *E* became the dominant one. Peak *B* appeared as a very narrow spike—characteristic of a phase transition. In the dried samples a similar spike appeared at 176° (peak *D*). The temperatures of both these

Table 1 Peak temperatures (°C) of DTA curves of non-dried and dried $MgCl_2$ recorded at different heating rates

Peak	Temperature, °C			
	Non-dried	Dried		
	10 deg/min	2 deg/min	10 deg/min	25 deg/min
A	101	75	95	100
B	115	118	118	118
C	154	127	150	193
D	n.d.	(176 sh)	176	178
E	184	153	185	223
F	240	200	234	270
G	440–480	431	462	500
H	715		715	715

n.d. – not detected; sh – shoulder.

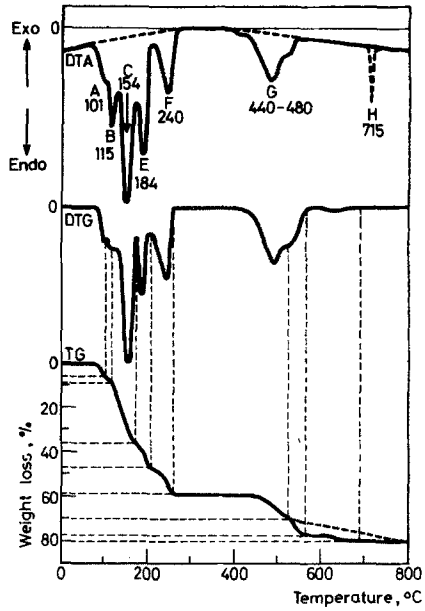

Fig. 1 DTA, DTG and TG curves of non-dried $MgCl_2 \cdot 6H_2O$

Table 2 Determination of Mg and Cl in samples heated to 400, 550, 800 and 1000 °C

Temperature, °C	Percentage		Molar ratio	
	Mg	Cl	Cl: Mg	O: Mg
400	30.8	50.5	1.12	
550	46.6	44.8	0.66	
800	62.0	0	0	0.93
1000	59.0	0	0	1.056

peaks remained unchanged with the heating rate, while the other peaks moved to higher temperatures with increasing heating rate (Table 1).

DTA and DTG peaks above 300°

All the samples were thermally stable between 275° and 400°. A complex endothermic DTA peak then began for both the dried and the non-dried samples, which appeared to be composed of two or three overlapping peaks, accompanied by a similar structure in the DTG curve. The reproducibility was poor and the temperature of the main peak varied between 440 and 480°. At higher temperatures, a gradual reduction in weight was observed, which in a static atmosphere

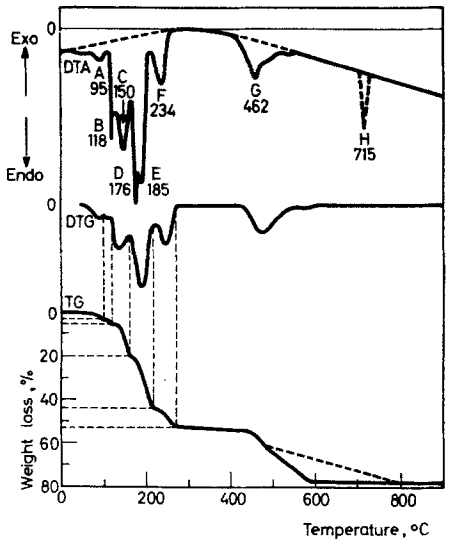

Fig. 2 DTA, DTG and TG curves of dried $MgCl_2 \cdot 6H_2O$

terminated at about 600° (with a total weight loss of about 80%). In flowing air, however, the weight decreased more slowly, and was stabilized at about 800° (dashed line in the TG curve of Figs 1 and 2). Whenever the weight reduction was not complete at 715°, a sharp DTA peak appeared at precisely that temperature (with no parallel DTG peak), which was probably due to the melting of anhydrous $MgCl_2$ [12].

Infrared spectra

The decomposition products of non-dried $MgCl_2 \cdot 6H_2O$, isolated at various stages of the thermal analysis, were investigated by infrared spectroscopy (Fig. 3). No hydroxyl groups were detected in the spectra of samples which were heated below 200°, showing that no significant hydrolysis took place below this temperature. Weak OH bands were detected in the spectrum of a sample heated to 215°. The intensity of the OH bands increased when the samples were heated to higher temperatures. The most intense OH bands were observed after the samples were heated at 400°. At 550° the bands became weaker. At this stage the decomposition products showed a high tendency to be hydrated (Fig. 3a), indicating the presence of amorphous phases. No OH bands were detected in the samples which had been heated to 800° or to higher temperatures. In this temperature range the spectrum of MgO was obtained. This thermal product did not show any tendency to retain water, indicating that at 800° the amorphous phases had been transformed into a crystalline phase.

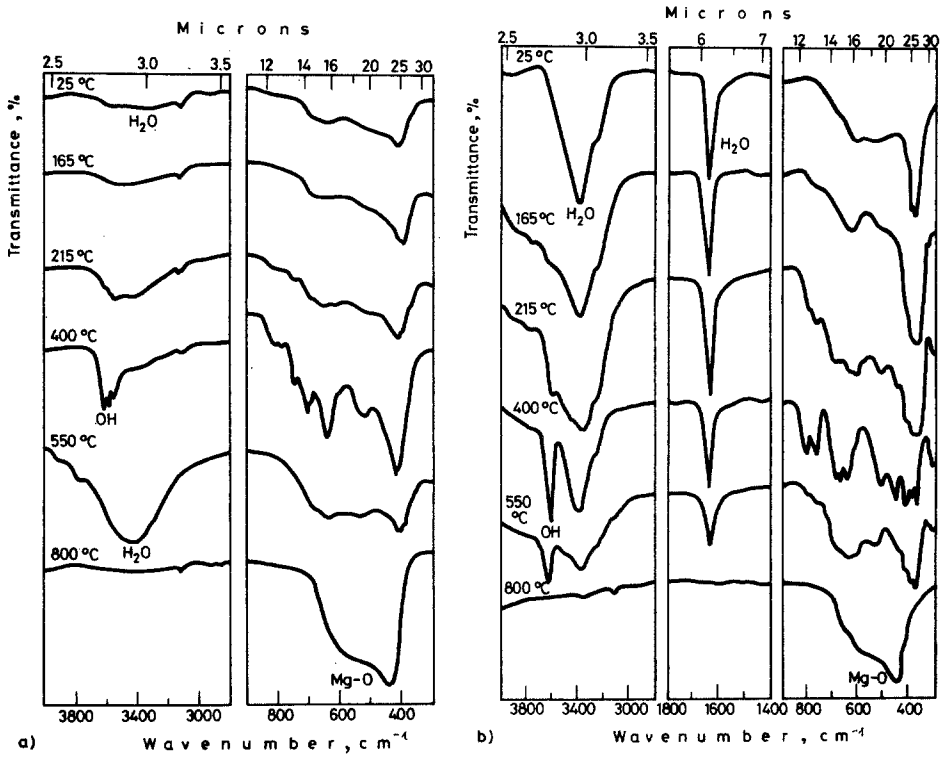

Fig. 3 Infrared spectra of thermal products of $MgCl_2 \cdot 6H_2O$, unheated (25°) and heated in the DTA furnace (heating rate 10 deg/min), to 165, 215, 400, 550 and 800 °C. (a) KBr disks dried at 350 °C, (b) CsCl disks dried at 250 °C

It has previously been shown that a solid solution of hydrated $MgCl_2$ is formed during grinding of this salt with CsCl [11]. This solid solution can be identified by a sharp absorption band at 1640 cm^{-1} (H_2O deformation), which is much broader when a solid solution is not formed. Neither MgO nor $Mg(OH)_2$ show this sharp band, which may therefore be used as an indication of the presence of $MgCl_2$ (hydrated or anhydrous). The intensity of this band decreased with the elevation of temperature, as shown in Fig. 3b, and the band was absent from the IR spectra of samples which had been heated to 800°.

There were significant differences between the shapes and locations of the OH stretching bands in KBr and CsCl disks. Three OH bands were detected in KBr disks, at 3515, 3565 and 3605 cm^{-1}, whereas only one band was detected in the CsCl disk, at 3616 cm^{-1}. These differences can be understood if one assumes that the OH groups form hydrogen-bonds with adsorbed water molecules. The strength of the hydrogen-bond depends on the inductive effect of the alkali metal halide

matrix. The fact that the OH groups are accessible to water molecules indicates that the magnesium hydroxy chlorides are non- or poorly-crystalline phases. This is also proved by the fact that these compounds are quite prominent in the IR spectra, but appear rather weakly in the X-ray diffractograms (see below), which are sensitive only to crystalline materials.

X-ray diffraction data

Samples heated to 400, 550, 800 and 1000° were examined by X-ray diffraction. The diffractograms are shown in Fig. 4.

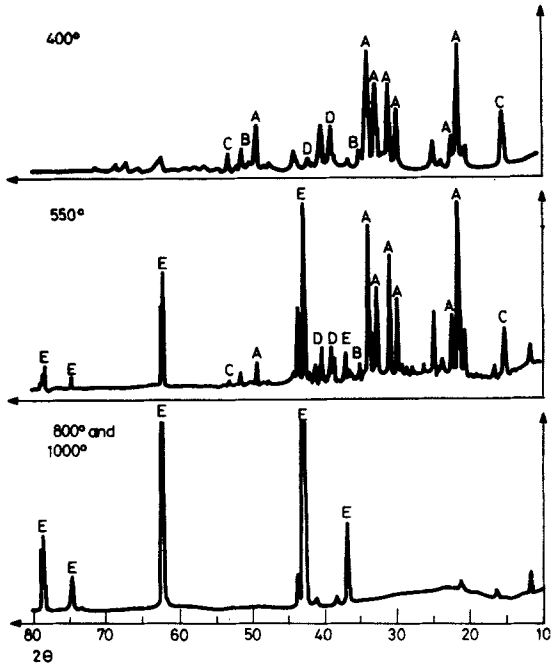

Fig. 4 X-ray diffractions of the thermal products of $MgCl_2 \cdot 6H_2O$ heated to 400 °C. (a) 550 °C (b) and 800 °C (c). A: $MgCl_2 \cdot 6H_2O$, B: $MgCl_2$, C: Mg(OH)Cl, D: $Mg(OH)_2Cl$, E: MgO

The diffractogram of the sample which had been heated to 400° revealed the presence of several Mg compounds. The most intense peaks were those of $MgCl_2 \cdot 6H_2O$. We assume that, initially, when the sample came out of the furnace, it contained anhydrous $MgCl_2$ or monohydrate, $MgCl_2 \cdot H_2O$, which was rehydrated during the period between the thermal treatment and the X-ray diffraction measurement. Indeed, small peaks of anhydrous $MgCl_2$ were also detected in the diffractograms (indicated *B* in Fig. 4). Several varieties of

magnesium hydroxy chloride were also found (*C* and *D*). Only the most intense peak of each compound appeared in the diffractogram, and the peaks were quite broad. These two facts indicate that the hydroxy phases were very badly crystallized, forming small crystals and amorphous material. Two different varieties of Mg(OH)Cl were identified, giving peaks at 575 and 172 pm. Two different varieties of $Mg_2(OH)_3Cl$ were identified as well, giving peaks at 230 and 223 pm (Fig. 4). Additional peaks indicated the presence of other phases which we did not succeed in identifying. They were probably various hydroxy phases having the general composition $Mg_x(OH)_yCl_{2x-y}$.

The diffractograms of the samples heated to 800° and 1000° are the same. The diffractograms demonstrated that these samples were composed of crystalline MgO. No other compounds were identified in these diffractograms.

The diffractogram of the sample heated to 550° showed all the peaks which were observed in the samples heated to 400°, or 1000°.

Chemical analysis

The Mg and Cl contents were determined in the non-dried samples which had been heated to 400, 550, 800 and 1000°. The results are given in Table 2. The Cl : Mg and O : Mg molar ratios are also presented in the Table. Since the Cl : Mg molar ratio for $MgCl_2 \cdot 6H_2O$ is 2, more than one-third of the Cl content is lost before the appearance of peak *G* in the DTA curve (Fig. 1). About one-third is lost during the appearance of peak *G* and the last portion is lost at higher temperature. The Table shows that MgO is the end-product of the thermal analysis. This is in agreement with the results of the X-ray and infrared studies.

Interpretation

The following reactions may occur in the course of the thermal analysis of $MgCl_2 \cdot 6H_2O$:

1. Dehydration

$$MgCl_2 \cdot xH_2O \rightarrow MgCl_2 \cdot (x-y)H_2O + yH_2O$$

2. Thermal hydrolysis

2a $\quad MgCl_2 \cdot H_2O \rightarrow Mg(OH)Cl + HCl$ or

2b $\quad 2MgCl_2 \cdot 3H_2O \rightarrow Mg_2(OH)_3Cl + 3HCl$ *etc.*

3. Dehydrochloridization or dehydroxylation

3a $\quad Mg(OH)Cl \rightarrow MgO + HCl$

3b $\quad Mg(OH)_2$ (amorphous) $+ MgCl_2 \rightarrow 2MgO + 2HCl$ or

3c $\quad 2Mg(OH)Cl \rightarrow MgO \cdot MgCl_2 + H_2O$ *etc.*

4. Melting.

Reactions 1–3 are associated with weight loss. The results obtained from TG, X-ray, infrared and chemical analysis, together with previous findings, can give information about the different reactions which occur in connection with the various DTA peaks.

According to Table 1, peaks *B*, *D* and *H* are independent of the heating rate. This is an indication that they represent melting of the phases $MgCl_2 \cdot 6H_2O$, $MgCl_2 \cdot 4H_2O$ and $MgCl_2$, respectively [2–6]. The other peaks shift to higher temperatures with rise in heating rate, and they are associated with weight loss.

Peak *A* in the DTA curve involves a weight loss of 5.5% for the non-dried samples and 3% for the dried one. This corresponds to the release of 0.65 and 0.32 mole water, respectively.

As pointed out by Buzágh–Gere et al. [3], the melting of the hexahydrate (peak *B*) is incongruent. They found that this phase transition occurs in an open crucible simultaneously with dehydration, while in a self-generated atmosphere it precedes the latter. It seems as if in the dried samples the release of water is hindered at low temperatures, even in an open crucible, and therefore peak *B* is very sharp, typical of a phase transition, while in the non-dried sample it is broadened due to overlapping with the dehydration process.

Peak *C* is also associated with weight loss. The infrared spectra of magnesium chloride heated up to 170° did not show any OH band. It is therefore concluded that dehydration is the principal reaction involved in this peak. This is in agreement with previous opinions [3–5, 10]. The TG of the non-dried salt showed a total weight loss of 36% for peaks *A*, *B* and *C*, which is equivalent to the loss of 4.2 mole H_2O per mole Mg. On the other hand, the TG of the dried salt showed a loss of 19–23%, which is equivalent to the loss of about 2.0–2.5 mole H_2O per mole Mg (Figs 1 and 2).

Peak *D* can probably be identified with the shoulder at 180°, which was attributed by Buzágh–Gere et al. to the melting of the tetrahydrate [3]. Most investigators did not detect this peak in their DTA curves. It was not detected in the DTA curve of the non-dried salt (Fig. 1), but was very sharp in the DTA curve of the dried salt.

Peak *E* represents further dehydration. The weight loss in this stage was 24 and 11 weight percent for dried and non-dried magnesium chloride, respectively. The appearance of small OH bands in the infrared spectra of samples taken from the DTA furnace after the completion of peak *E* (215°) indicates that thermal hydrolysis starts at this stage, but contributes only little to the weight loss.

The differences between Figs 1 and 2 can be interpreted if one assumes that the dried magnesium chloride contains a mixture of $MgCl_2 \cdot 4H_2O$ and $MgCl_2 \cdot 6H_2O$ crystals, whereas the non-dried salt contains only $MgCl_2 \cdot 6H_2O$ crystals plus humidity. Peaks *A* and *C* are characteristic of the hexahydrate and are therefore more intense in the curves of the non-dried salt. It is suggested that the dihydrate is

the principal dehydration product of the molten hexahydrate. According to the TG curve, this is obtained during the appearance of peak *C*. Only small amounts of the tetrahydrate were obtained at this stage in the non-dried samples, and this may be dissolved in the liquid phase obtained with peak *B*. Consenquently, peak *D*, which is associated with the melting of the tetrahydrate, was not detected in the DTA curve of the non-dried salt and peak *E* is weak. However, both peaks were very intense in the curve of the dried salt, which initially contained the tetrahydrate besides the hexahydrate.

The infrared spectra of samples heated to 270 or 400° exhibited very intense OH bands. This is an indication that thermal hydrolysis (reactions 2a and 2b above) is the principal reaction which is associated with peak *F*. X-ray data showed that several varieties of magnesium hydroxy chloride were produced with a very low degree of crystallinity. These amorphous phases are surface-active and may hold adsorbed water to temperatures exceeding that of peak *G*. Chemical analysis showed that at 400°, 43.85% of the chlorine had been liberated as HCl.

The infrared and X-ray diffraction spectra of samples heated to 500 or 550° revealed a decrease in the intensity of the OH bands and the appearance of MgO. Chemical analysis showed that at this stage 66.6% of the chlorine was liberated as HCl. This is an indication that dehydrochloridization started with peak *G*. The dehydrochloridization was a relatively slow reaction and it continued up to 600° in static air or up to 800° in flowing air. Infrared, X-ray and chemical analysis data indicated that MgO was the only end-product of the thermal analysis. The dehydrochloridization which occurred at this stage seems to be a complicated reaction, accompanied by recrystallization and crystal growth. Consequently, peak *G* was broad and had an irregular shape.

The appearance of peak *H* in the DTA curve reveals the presence of anhydrous $MgCl_2$. This peak appeared if the DTA was carried out in flowing air, and it did not appear in a static atmosphere. It was previously mentioned that in static air the weight-losing process terminated at 600° and no $MgCl_2$ was left in the crucible to give peak *H*. In flowing air, on the other hand, the weight-losing process terminated only at about 800°.

The appearance of peak *H* indicated that $MgCl_2$ was still present in the crucible. No parallel exothermic peak was observed in a DTA cooling curve recorded from 1000° to room temperature. Consequently, it was concluded that $MgCl_2$ was present in the system as long as weight loss was observed. This was also proved from the spectra of the thermal decomposition products recorded in CsCl disks. The anhydrous $MgCl_2$ finally reacts with the H_2O gas formed in the dehydroxylation of the magnesium hydroxy chloride (Eq. 3c above), to give MgO as the ultimate product of the heating: $MgCl_2(s) + H_2O(g) \rightarrow MgO(s) + 2HCl(g)$

Kinetic parameters

All the DTA and DTG peaks, except those which are evidently associated with phase transitions (peaks *B* and *D* for the dried samples and *H* for both the dried and non-dried samples), were analyzed by assuming the validity of the rate equation: $d\alpha/dt = k(1-\alpha)^b$. In this equation, α is the fraction of the sample which has been decomposed, b is the apparent reaction order, and the rate constant k is given by the Arrhenius equation: $k = A \cdot \exp(-E/RT)$, E being the activation energy, A the frequency factor, R the gas constant and T the temperature (in K). The parameters E, b and A were calculated by using three methods.

a) In the *initial rate method,* $\ln I$ is plotted against $1/T$ for the low-temperature part of the peak, where I is the intensity of the DTA or DTG signal. This should yield a straight line, the slope of which is $-E/R$. For each peak 5–10 points were taken and E was calculated through numerical least-square fitting on a microcomputer.

b) According to *Freeman and Carroll* [13], a plot of $\Delta \ln(d\alpha/dT)/\Delta \ln(1-\alpha)$ against $\Delta(1/T)/\Delta \ln(1-\alpha)$ should give a straight line with a slope of $-E/R$ and an intercept of b at the y axis (Δ represents the difference between two points on the curve). Ten to twenty data points were taken for each peak. The intensity I represented $d\alpha/dt$, while α was computed by numerical integration. Here too, the parameters E and b were calculated by a microcomputer. Freeman–Carroll curves for DTA and DTG peaks of a non-dried sample are shown in Fig. 5.

c) In *Chen's half-width method* [14, p. 159], which was originally developed for thermoluminescence but can be applied to DTG and DTA as well, three points on the peak are used: the maximum temperature T_m, and T_1 and T_2, the low and high half-intensity temperatures, respectively (see Fig. 6). Three parameters, ω, τ and δ, are defined by $\omega = T_2 - T_1$, $\tau = T_m - T_1$ and $\delta = T_2 - T_m$. The reaction order is evaluated by using the ratio $\mu = \delta/\omega$. It was found by analyzing "synthetic" peaks that for $b = 0.5$, 1.0, 1.5, 2.0 and 2.5 the values of μ are 0.332, 0.423, 0.485, 0.524 and 0.555, respectively. Using these figures, one can compute b (for $0 < b < 3$) by interpolation or extrapolation. The activation energy is given by the equation:

$$E = A_\omega RT_m^2/\omega - B_\omega 2RT_m$$

where $B_\omega = 1$ and A_ω is 2.5 for $b = 1$ and 3.54 for $b = 2$. For other b values E can be evaluated by linear interpolation or extrapolation between $E(b = 1)$ and $E(b = 2)$. Similar equations exist for τ and δ. A_τ and B_τ are 1.51 and 1.58, respectively, for first order, and 1.81 and 2 for second order. $B_\delta = 0$ and A_δ is 0.976 for $b = 1$ and 1.71 for $b = 2$.

For peaks which happened to be "clean" on both sides, we took the average of E_ω, E_τ and E_δ as the activation energy. When overlapping occurred on the low- or high-temperature side, only one quantity (E_δ or E_τ) could, of course, be evaluated.

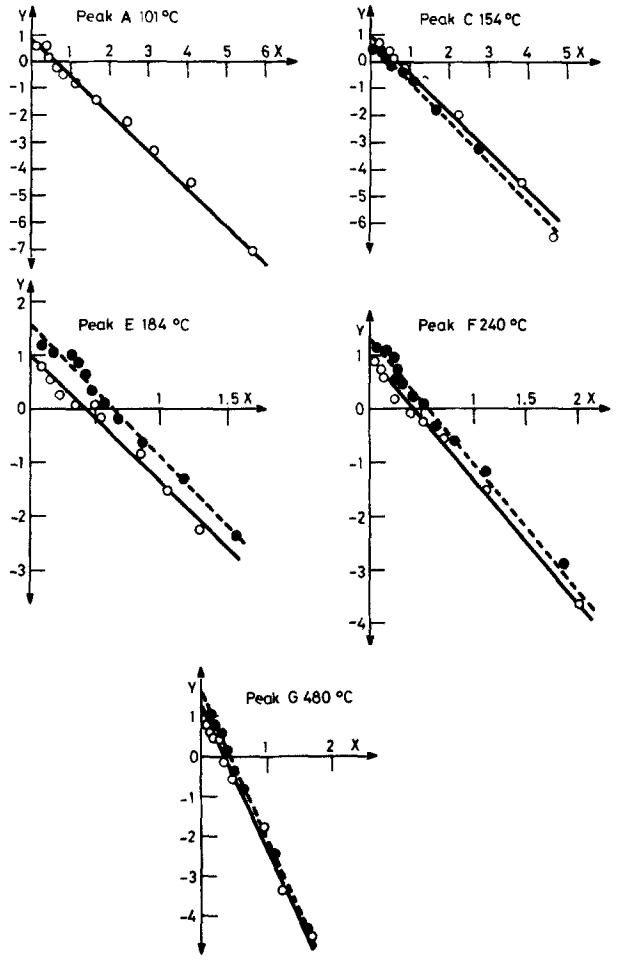

Fig. 5 Freeman–Carroll curves for DTG and DTA peaks of non-dried $MgCl_2 \cdot 6H_2O$. – ○ – DTG, – – ● – – DTA

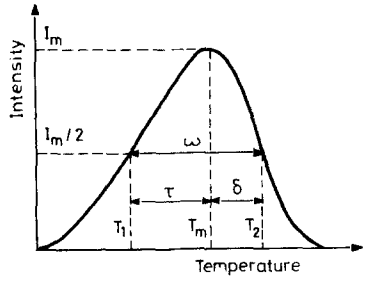

Fig. 6 The parameters used in Chen's method for evaluating E and b

It should be mentioned that theoretically all these methods are applicable to DTG, but not to DTA peaks, since the DTA signal is not exactly proportional to the reaction rate $d\alpha/dt$, but rather to $d\alpha/dt+(C/K)d^2\alpha/dt^2$, where C is the heat capacity of the sample and K is the heat transfer coefficient [14, p. 109]. However, in our case (small samples in an open sample holder) the error arising from using these methods with DTA was found to be very small.

The kinetic data obtained by applying the various methods to the non-dried samples are summarized in Table 3. Each figure in the Table is the average of several runs. In most cases the distribution of the results was small (less than 5%), with the exception of Chen's activation energy for peak *A* and the reaction order for some of the peaks for which the ranges of the results are given rather than the means. Overlapping prevented us from applying the Freeman–Carroll or the initial rate method to some of the peaks. In peak *B* neither method could be used due to strong overlapping, and only Chen's method was applied.

Table 3 Kinetic parameters of the DTA and DTG peaks of non-dried $MgCl_2 \cdot 6H_2O$ evaluated by the methods of Freeman and Carroll (F.C.) and Chen, and by the initial rate method (I.R.)

Peak	Temperature, °C	Activation energy, kJ·mole^{-1}						Reaction order (b)			
		DTA			DTG			DTA		DTG	
		F.C.	Chen	I.R.	F.C.	Chen	I.R.	F.C.	Chen	F.C.	Chen
A	101	—	117–146	111	114	123–163	116	—	0.5–1.5	0.8	0.5
B	115	—	272	—	—	—	—	—	2	—	—
C	154	126	131	—	131	124	—	1	1	1	1
E	184	209	188	—	197	209	—	1.6	1	1	1–2
F	240	218	213	210	210	188	223	1–1.5	1	1	0.5
G	480	314	310	300	297	301	295	1.3	1.5	1–1.5	1.5

The averages of the parameters E and b obtained by the various methods are presented in Table 4. E is given in kcal·mole^{-1} as well, and the pre-exponential factor A is computed using the relation [14]:

$$\beta A^{-1} = \exp\left(-\frac{E}{RT_m}\right)\left(\frac{bRT_m^2}{E}-(b-1)\frac{RT_m^2}{E+2RT_m}\right)$$

where β is the heating rate (deg·sec^{-1}) and T_m is the peak temperature (in K).

Applying the same methods to peak *A*, *E*, *F* and *G* for the dried samples, we found values which were very close to those presented in Table 4; the activation energy of peak *C* appeared to be about 20% lower than the value in Table 4. However, since this peak for the dried sample is strongly overlapped on both sides, the result is not very reliable, and one can take the values appearing in Table 4 as representing the

Table 4 Average values of the parameters E, A and b

Peak	Temperature, °C	Activation energy, E		A, sec^{-1}	b
		$kJ \cdot mole^{-1}$	$kcal \cdot mole^{-1}$		
A	101	115	27.5	1.9×10^{14}	0.8
B	115	272	65.0	1.5×10^{35}	2
C	154	128	30.6	6.5×10^{13}	1
E	184	201	48.0	1.8×10^{21}	1–1.5
F	240	210	50.3	3.9×10^{19}	1
G	480	303	72.4	1.1×10^{19}	1.5

dried samples as well (except for peak *B*, which for the dried samples appears as a narrow phase-transition peak which is not describable in terms of the Arrhenius equation).

The activation energies for peaks *A* and *C* are 27.5 and 30.6 $kcal \cdot mole^{-1}$, respectively. The activation energy of *C* is typical of dehydration processes preceded by melting. Buzágh–Gere et al. [15] found a similar value (28 $kcal \cdot mole^{-1}$) for the activation energy of the release of the first 5 water molecules from $SrBr_2 \cdot 6H_2O$, which occurs through incongruent melting. They also found that activation energies of dehydration processes not accompanied by the formation of liquid phase are typically higher—between 34 and 66 $kcal \cdot mole^{-1}$ [15]. In another work, Buzágh–Gere et al. [1] assign activation energies of 17.2 and 36.0 $kcal \cdot mole^{-1}$ to the first two dehydration steps of $MgCl_2 \cdot 6H_2O$. In comparing those values with our data, one has to remember that kinetic parameters of thermal processes are empirical quantities which are dependent on the experimental conditions. Further work is needed to establish the dependence of the kinetic parameters on the external conditions in this case.

The abnormally high E and A values for peak *B* stem from the fact that this peak is quite narrow even for the non-dried samples, showing that the dominant process here too is melting. Actually, this makes the kinetic parameters meaningless, since a phase transition is not suitable for this sort of analysis.

The higher values of E and A found for peaks E and F (201 and 210 $kJ \cdot mole^{-1}$, respectively) reflect the fact that the last two water molecules are more strongly bound, and that hydrolysis processes are acting here as well. More work is needed to find out which process, or processes, provides the observed value of 303 $kJ \cdot mole^{-1}$ associated with peak *G*.

Conclusions

The dried magnesium chloride contains a mixture of $MgCl_2 \cdot 4H_2O$ and $MgCl_2 \cdot 6H_2O$ crystals, whereas the non-dried salt contains only $MgCl_2 \cdot 6H_2O$ plus humidity. The thermal analysis of non-dried and dried magnesium chloride provides eight endothermic peaks. Although several reactions may occur simultaneously, it is possible to attribute certain peaks to certain reactions. Three peaks (*B*, *D* and *H*) can be attributed to the melting of $MgCl_2 \cdot 6H_2O$, $MgCl_2 \cdot 4H_2O$ and $MgCl_2$. Three peaks (*A*, *C* and *E*) are associated mainly with dehydration. One peak (*F*) is associated mainly with thermal hydrolysis, and one peak (*G*) is associated with dehydrochloridization. It seems that $MgCl_2 \cdot 2H_2O$ is the principal dehydration product of the hexahydrate, being formed during the appearance of peak *C*. The monohydrate is formed during the appearance of peak *E* by the dehydration of either $MgCl_2 \cdot 4H_2O$ or $MgCl_2 \cdot 2H_2O$. The activation energy of the dehydration processes increases with decreasing hydration number of the Mg. The activation energy of the hydrolysis is higher than that of dehydration. The dehydrochloridization is the most complicated process occurring during the thermal analysis, and is accompanied by recrystallization and crystal growth. This stage has a very high activation energy.

* * *

The authors express their appreciation to Dr. Jacob Nathan and Mr. Yoetz Deutch from the Geological Survey, Jerusalem, for the use of the thermal analysis instrument and for useful discussion, and to Mrs. Sarah Erlich from the same institute, for the chemical analysis. The financial support by Everyman's University, Tel-Aviv, and by the Hebrew University of Jerusalem is acknowledged.

References

1 É. Buzágh-Gere, S. Gál and J. Simon, in H. G. Wiedemann "Thermal Analysis." Proc. III ICTA, 1971, Vol. 2, Birkhauser Verlag, Basel 1972, p. 635.
2 É. Buzágh-Gere, S. Gál and J. Simon, Z. Anorg. Allg. Chem., 400 (1973) 37.
3 É. Buzágh-Gere, S. Gál and J. Simon, Hungarian Sci. Inst., 28 (1973) 25.
4 K. Heide and H. J. Eichhorn, J. Thermal Anal., 7 (1975) 397.
5 D. Petzold and R. Naumann, J. Thermal Anal., 19 (1980) 25.
6 T. J. Gardner and G. L. Messing, Thermochim. Acta, 78 (1984) 17 and F. H. Herbstein, M. Kapon and A. Weisman, Isr. J. Chem., 22 (1982) 207.
7 Y. Kato and K. Tachiki, J. Soc. Chem. Ind. Japan Suppl., 31B (1928) 104.
8 G. Grube and W. Brauning, Z. Elektrochem. Angew. Phys. Chem., 44 (1938) 134.
9 L. G. Berg and N. P. Burmistrova, Zh. Neorgan. Khim., 5 (1960) 676.
10 L. G. Berg, Ch. II in R. C. Mackenzie "Differential Thermal Analysis", Vol. 1, Academic N.Y. 1970, p. 355.
11 S. Shoval and S. Yariv, Thermochim. Acta, 92 (1985) 819.
12 R. C. Weast and M. J. Astle, eds., CRC Handbook of Chemistry and Physics, 1979.

13 E. S. Freeman and B. J. Carroll, Phys. Chem., 62 (1958) 394.
14 R. Chen and Y. Kirsh, "Analysis of Thermally Stimulated Processes;" Pergamon, Oxford, 1981.
15 É. Buzágh-Gere, J. Simon and S. Gál, Z. Anal. Chem., 264 (1973) 392.
16 S. Shoval, Y. Yariv, Y. Kirsh and H. Peled, Thermochim. Acta, 109 (1986) 207.

Zusammenfassung — Die thermische Zersetzung von $MgCl_2 \cdot 6H_2O$ (nicht und teilweise getrocknet) und die Kinetik dieses Prozesses wurden mittels DTA, TG, DTG, IR, Röntgendiffraktometrie und chemischer Analyse von Mg und Cl untersucht. Die im Verlaufe der thermischen Analyse vor sich gehenden Reaktionen sind Dehydratisierung (in Schritten), thermische Hydrolyse von $MgCl_2 \cdot H_2O$ und Chlorwasserstoffaustritt aus Magnesiumhydroxychloriden. Das Schmelzen der Phasen $MgCl_2 \cdot 6H_2O$, $MgCl_2 \cdot 4H_2O$ und $MgCl_2$ ist in den thermischen Kurven ebenfalls zu erkennen. Im Luft- und Stickstoffstrom erfolgt ein Gewichtsverlust bis 800 °C, in statischer Luftatmosphäre dagegen nur bis 700 °C. MgO war in beiden Fällen Endprodukt der thermischen Behandlung. Die kinetischen Parameter der Reaktion (Aktivierungsenergie E, präexponentieller Faktor A, scheinbare Reaktionsordnung b) wurden nach verschiedenen Methoden berechnet. Aktivierungsenergie und scheinbare Reaktionsordnung der Dehydratisierung nehmen mit abnehmendem Hydratationsgrad des Mg zu. Die Chlorwasserstoffabspaltung erfordert die höchste Aktivierungsenergie.

Резюме — Методом ДТА, ТГ, ДТГ, ИК спектроскопии, рентгеноструктурного анализа и химического анализа было изучено термическое разложение гексагидрата хлористого магния (влажного и частично высушенного) и кинетика процесса его разложения. Были идентифицированы следующие реакции: дегидратация (ступенчатая), термический гидролиз моногидрата хлорида магния и дегидрохлорирование основной соли магния. На термических кривых идентифицированы температуры плавления гексагидрата, тетрагидрата хлорида магния и безводной соли. В динамической атмосфере воздуха и азота термическая потеря веса продолжалась до температуры 800 °C, тогда как в статической атмосфере воздуха — до 700 °C. В обоих случаях конечным продуктом разложения являлась окись магния. Несколькими методами были расчитаны энергия активации, предэкспоненциальный множитель и кажущийся порядок реакции. Установлено, что энергия активации и кажущийся порядок реакции дегидратации увеличиваются с уменьшением числа гидратации магния. Процесс дегидрохлорирования имел наиболее высокое значение энергии активации.